

***Supplementary Material***

**Cu(II) complexes with tridentate sulfur and selenium ligands: catecholase and  
hydrolysis activity**

by

**Daniele Cocco Durigon<sup>a</sup>, Marcos Maragno Peterle<sup>a</sup>, Adailton João Bortoluzzi<sup>a</sup>, Ronny  
Rocha Ribeiro<sup>b</sup>, Antonio Luiz Braga<sup>a</sup>, Rosely Aparecida Peralta<sup>a\*</sup>, Ademir Neves<sup>a\*</sup>**

<sup>a</sup> Departamento de Química, Universidade Federal de Santa Catarina, Florianópolis – SC,  
Brazil. CEP 88040-900.

<sup>b</sup> Departamento de Química, Universidade Federal do Paraná, Curitiba – PR, Brazil. CEP  
81531-980

\*Corresponding author: [ademir.neves@ufsc.br](mailto:ademir.neves@ufsc.br); [rosely.peralta@ufsc.br](mailto:rosely.peralta@ufsc.br)

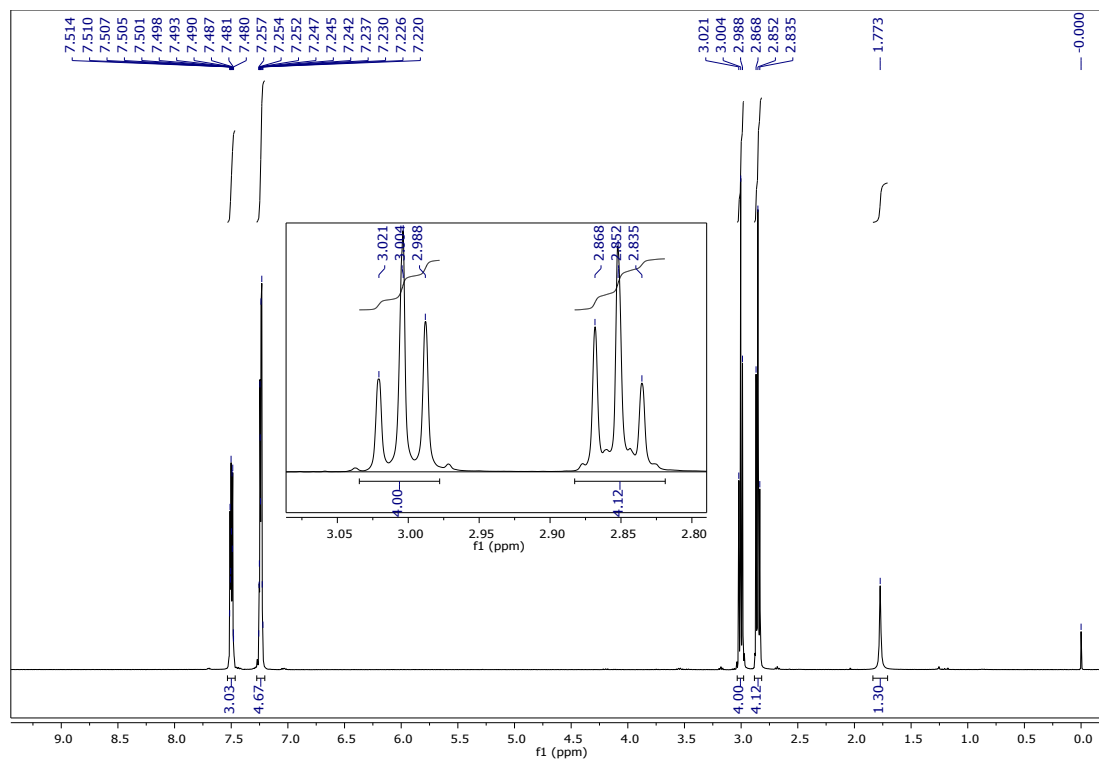


Figure S1  $^1\text{H}$  NMR (400 MHz,  $\text{CDCl}_3$ ) spectrum of  $\text{L}_{\text{se}}$ .

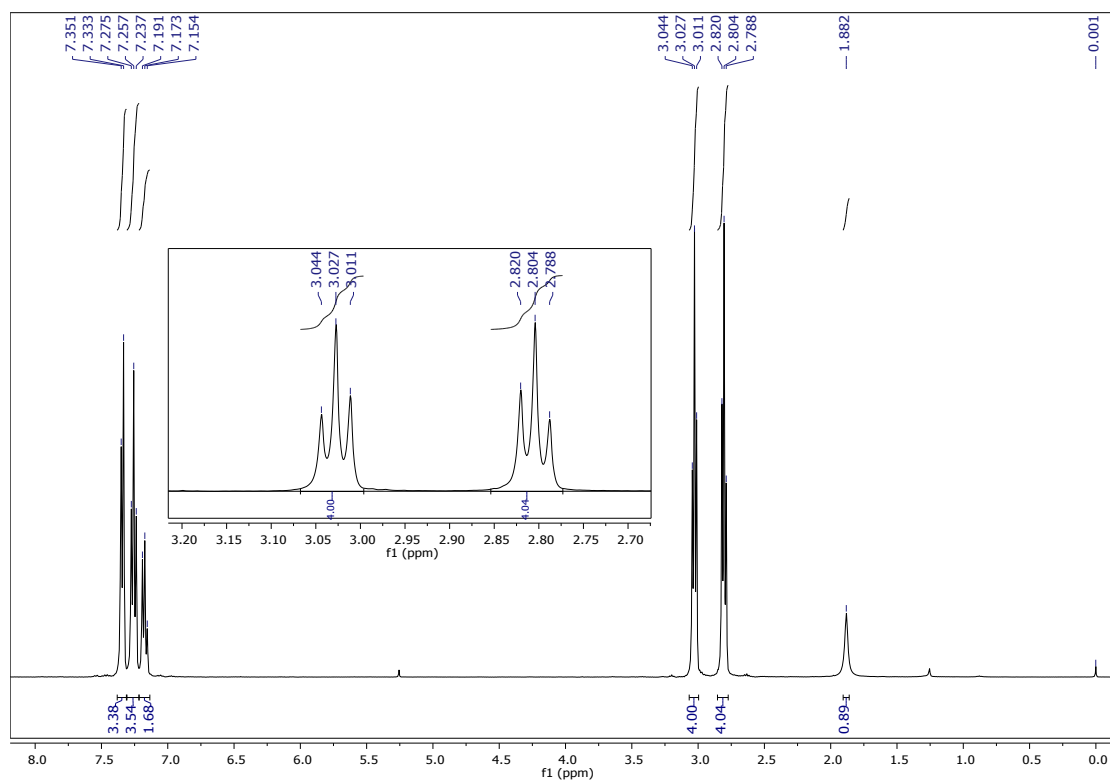


Figure S2  $^1\text{H}$  NMR (400 MHz,  $\text{CDCl}_3$ ) spectrum of  $\text{L}_{\text{s}}$ .

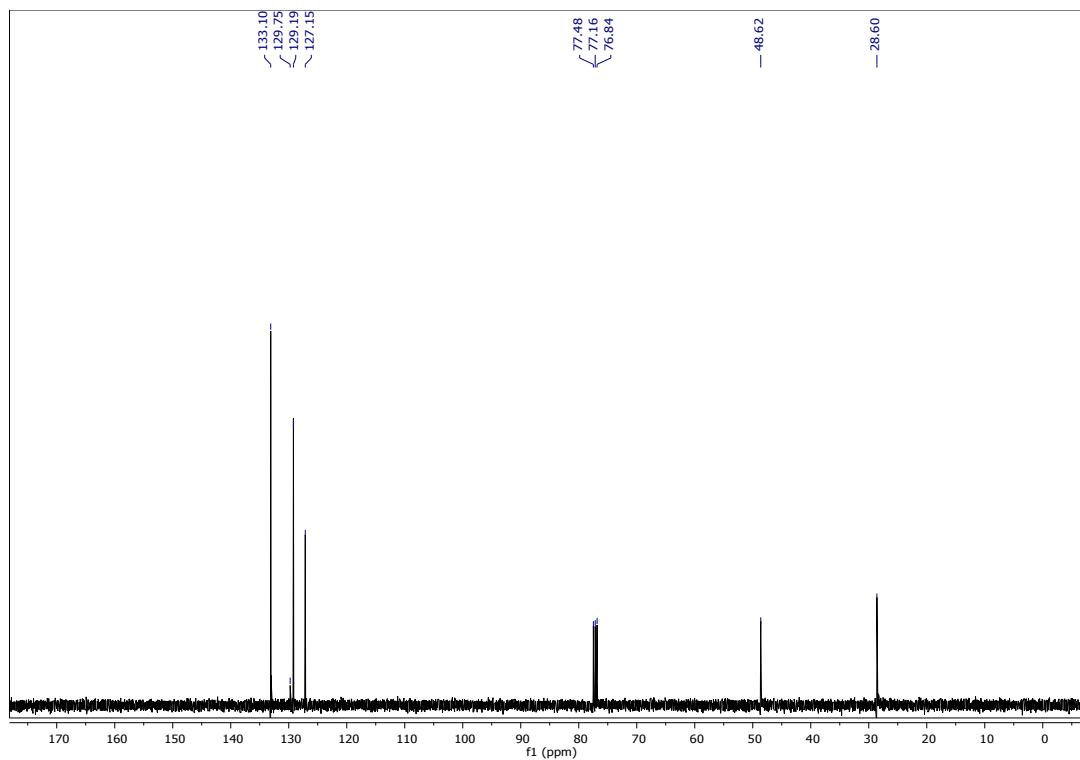


Figure S3  $^{13}\text{C}$  NMR (100 MHz,  $\text{CDCl}_3$ ) spectrum of  $\text{L}_{\text{Se}}$ .

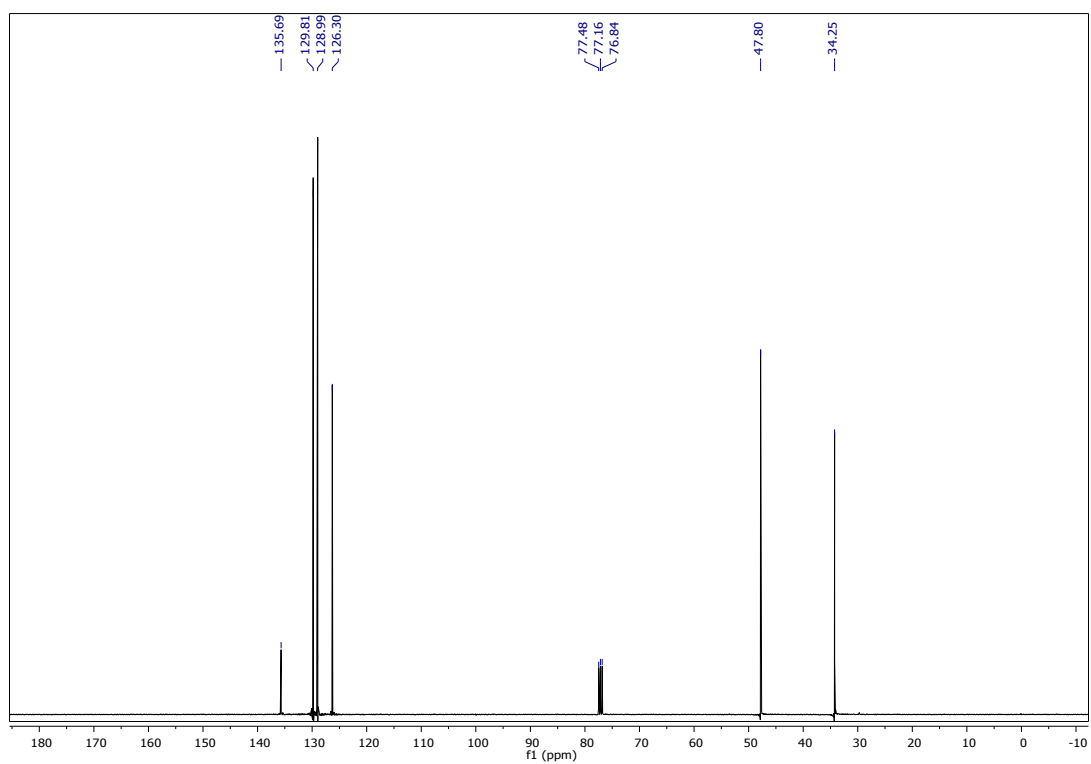


Figure S4  $^{13}\text{C}$  NMR (100 MHz,  $\text{CDCl}_3$ ) spectrum of  $\text{L}_{\text{S}}$ .

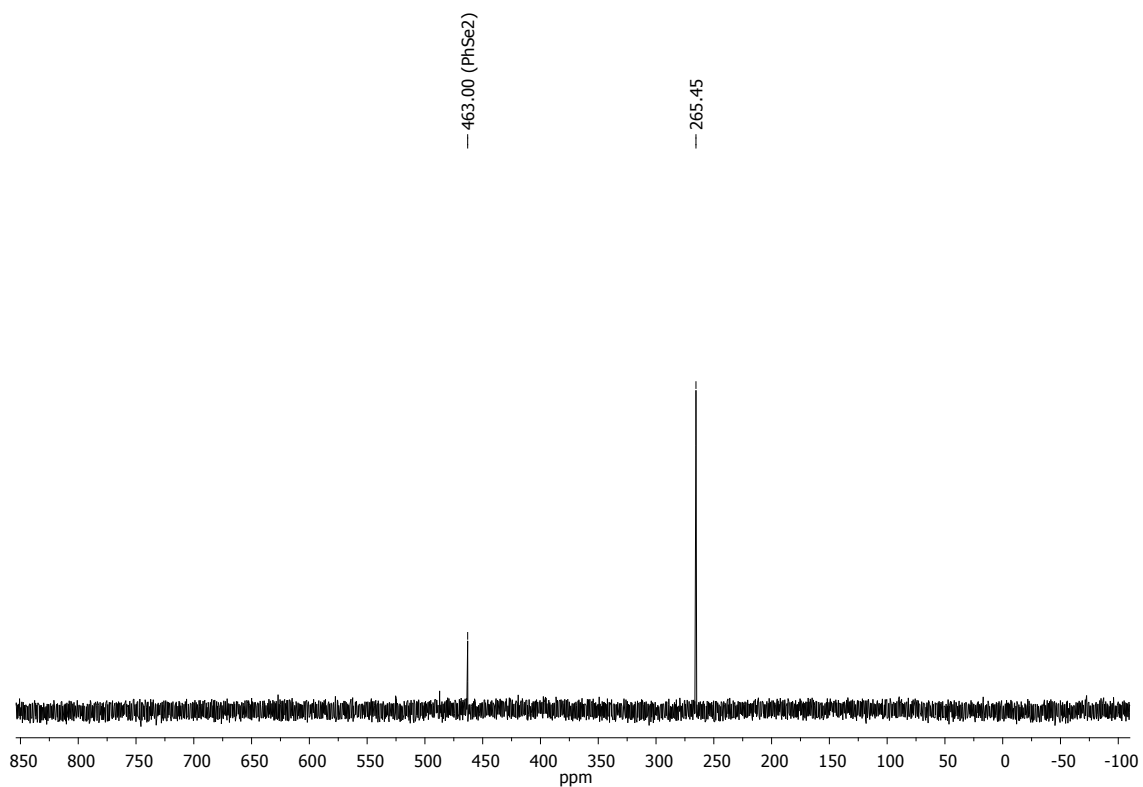


Figure S5  $^{77}\text{Se}$  NMR (76 MHz,  $\text{CDCl}_3$ ) spectrum of  $\text{L}_{\text{Se}}$ .

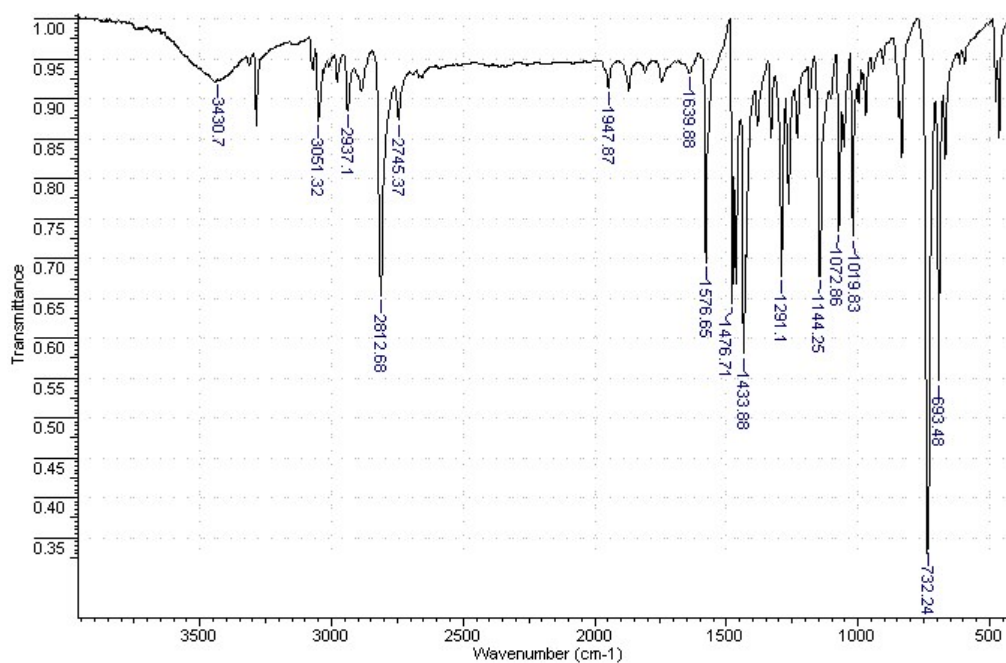


Figure S6 IR (KBr,  $\text{cm}^{-1}$ ) of  $\text{L}_{\text{Se}}$ .

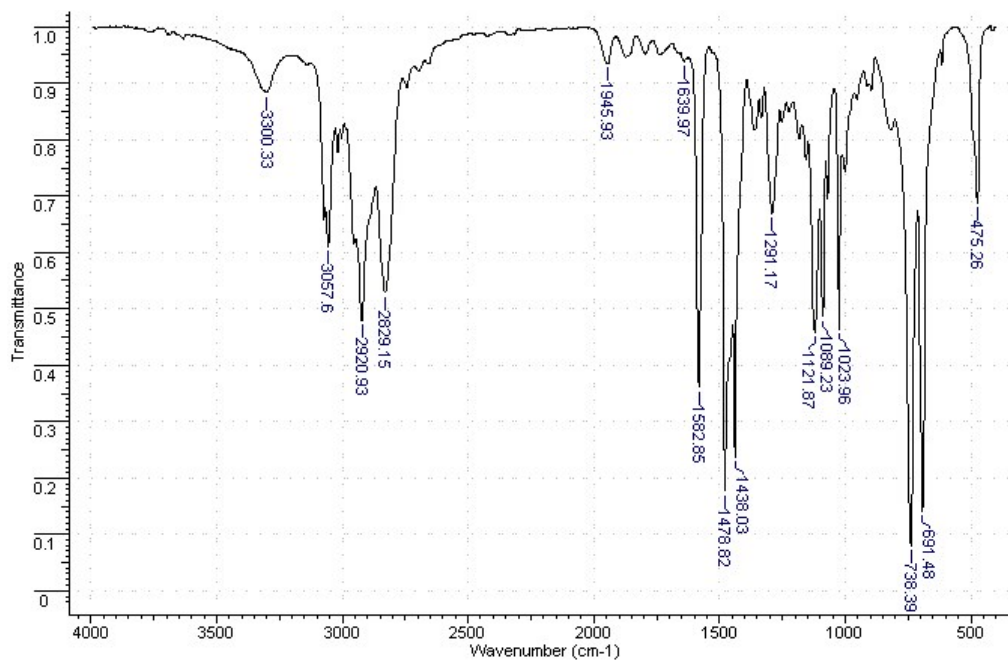


Figure S7 IR (KBr,  $\text{cm}^{-1}$ ) of  $L_5$ .

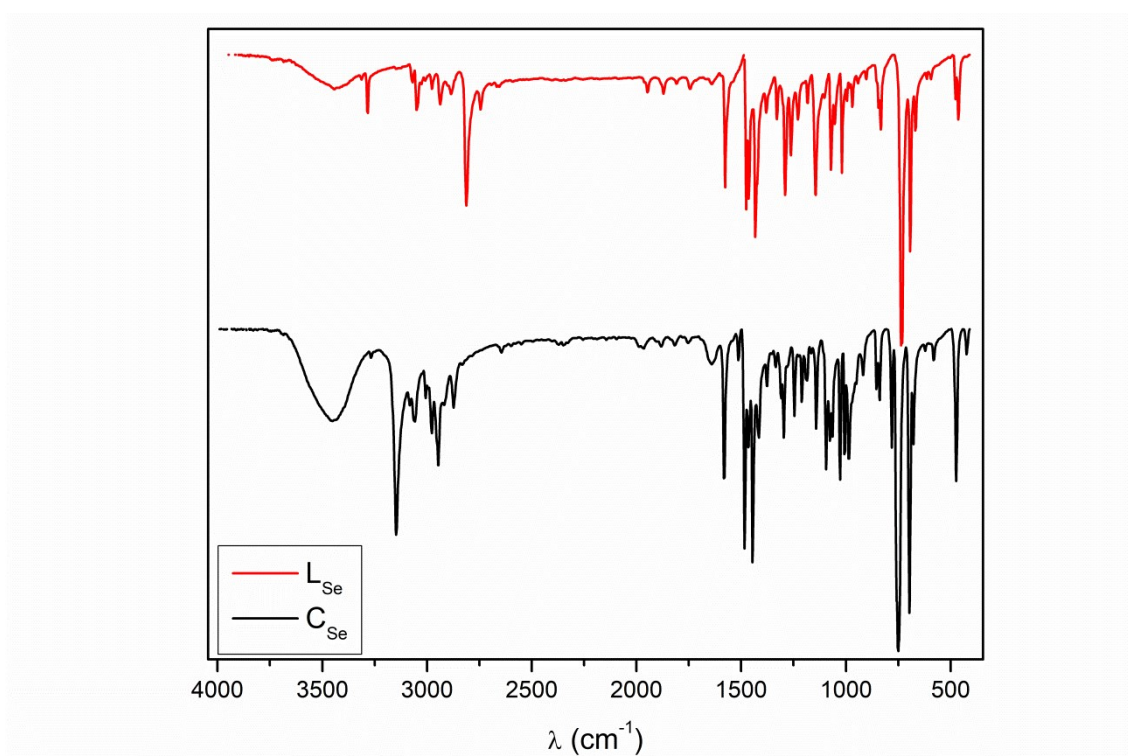
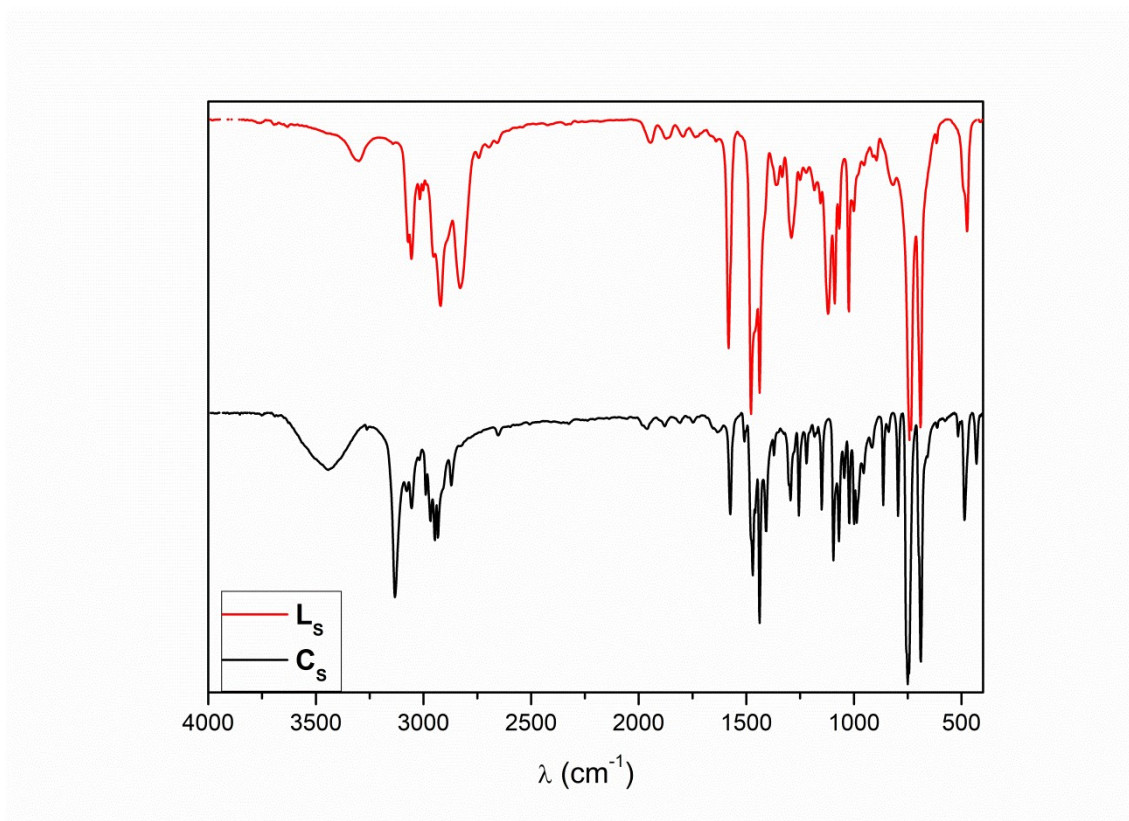


Figure S8 IR spectra overlay of the  $L_{Se}$  (red) and  $C_{Se}$  (black).



**Figure S9** IR spectra overlay of the  $L_s$  (red) and  $C_s$  (black).

### Crystallographic Data

**Table S1** Bond lengths (Å) and angles (°) for  $C_{Se}$ .

Cu1-N1	2.036(3)	C1-C2	1.516(3)
Cu1-Cl1	2.2411(9)	C1-H1A	0.9900
Cu1-Cl2	2.4076(8)	C1-H1B	0.9900
Cu1-Se1	2.5196(3)	C2-Se1	1.968(2)
Cu1-Se1 <sup>i</sup>	2.5196(3)	C2-H2A	0.9900
N1-C1 <sup>i</sup>	1.472(3)	C2-H2B	0.9900
N1-C1	1.473(3)	Se1-C3	1.925(2)
N1-H1	0.8718	C3-C4	1.384(3)
C3-C8	1.385(3)	C7-H7	0.9500
C4-C5	1.385(3)	C8-H8	0.9500
C4-H4	0.9500	N1-Cu1-Cl1	164.62(8)
C5-C6	1.385(4)	N1-Cu1-Cl2	96.72(8)
C5-H5	0.9500	Cl1-Cu1-Cl2	98.66(3)

C6-C7	1.382(4)	N1-Cu1-Se1	82.36(3)
C6-H6	0.9500	Cl1-Cu1-Se1	92.312(13)
C7-C8	1.389(4)	Cl2-Cu1-Se1	110.164(10)
N1-Cu1-Se1 <sup>i</sup>	82.36(3)	Cu1-N1-H1	105.3
Cl1-Cu1-Se1 <sup>i</sup>	92.312(13)	N1-C1-C2	108.31(19)
Cl2-Cu1-Se1 <sup>i</sup>	110.164(10)	N1-C1-H1A	110.0
Se1-Cu1-Se1 <sup>i</sup>	138.154(19)	C2-C1-H1A	110.
C1 <sup>i</sup> -N1-C1	114.2(2)	N1-C1-H1B	110.0
C1 <sup>i</sup> -N1-Cu1	111.67(14)	C2-C1-H1B	110.0
C1-N1-Cu1	111.67(14)	H1A-C1-H1B	108.4
C1 <sup>i</sup> -N1-H1	106.7	C1-C2-Se1	111.00(15)
C1-N1-H1	106.7	C1-C2-H2A	109.4
Se1-C2-H2A	109.4	C3-Se1-C2	99.13(10)
C1-C2-H2B	109.4	C3-Se1-Cu1	113.30(7)
Se1-C2-H2B	109.4	C2-Se1-Cu1	93.56(7)
H2A-C2-H2B	108.0	C4-C3-C8	120.2(2)
C4-C3-Se1	123.16(17)	C6-C5-H5	119.7
C8-C3-Se1	116.59(19)	C7-C6-C5	119.6(3)
C3-C4-C5	119.6(2)	C7-C6-H6	120.2
C3-C4-H4	120.2	C5-C6-H6	120.2
C5-C4-H4	120.2	C6-C7-C8	120.2(3)
C4-C5-C6	120.6(3)	C6-C7-H7	119.
C4-C5-H5	119.7	C8-C7-H7	119.9
C3-C8-C7	119.8(3)	C7-C8-H8	120.1
C3-C8-H8	120.1		

Symmetry transformations used to generate equivalent atoms: (i) X, -Y+1.5, Z.

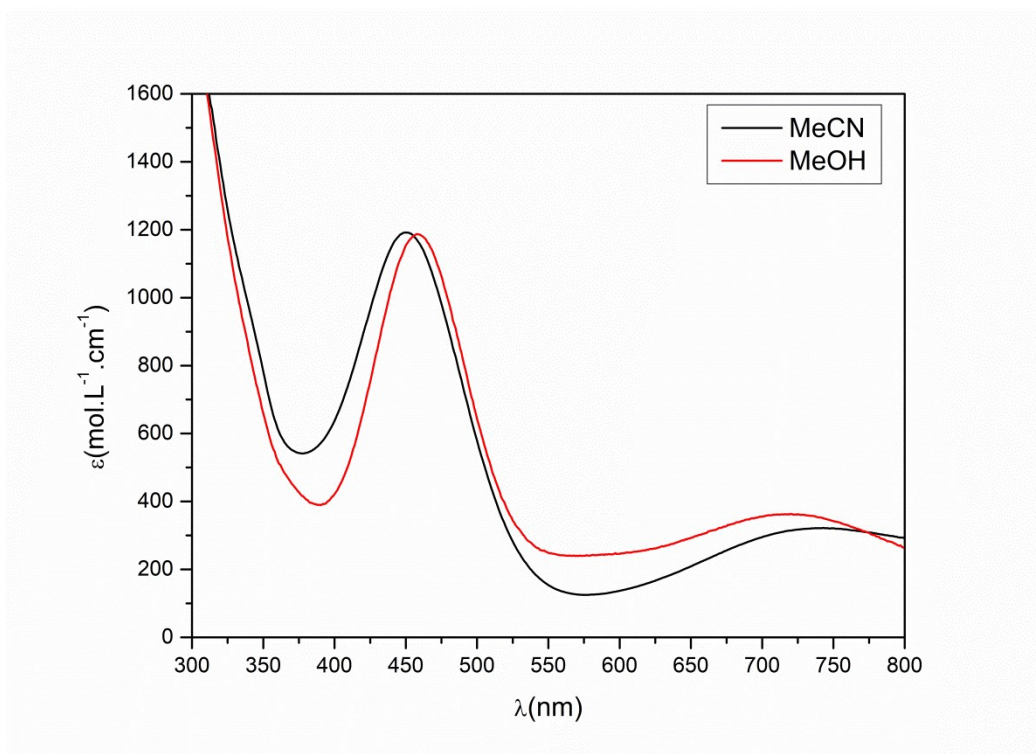
**Table S2** Bond lengths (Å) and angles (°) for C<sub>5</sub>

Cu1-N1	2.0141(18)	C3-C8	1.393(2)
Cu1-Cl1	2.2284(6)	C4-C5	1.391(2)
Cu1-Cl2	2.4100(6)	C4-H4	0.9500
Cu1-S1	2.4500(4)	C5-C6	1.382(3)
Cu1-S1 <sup>i</sup>	2.4501(4)	C5-H5	0.9500
N1-C1	1.4769(18)	C6-C7	1.382(3)

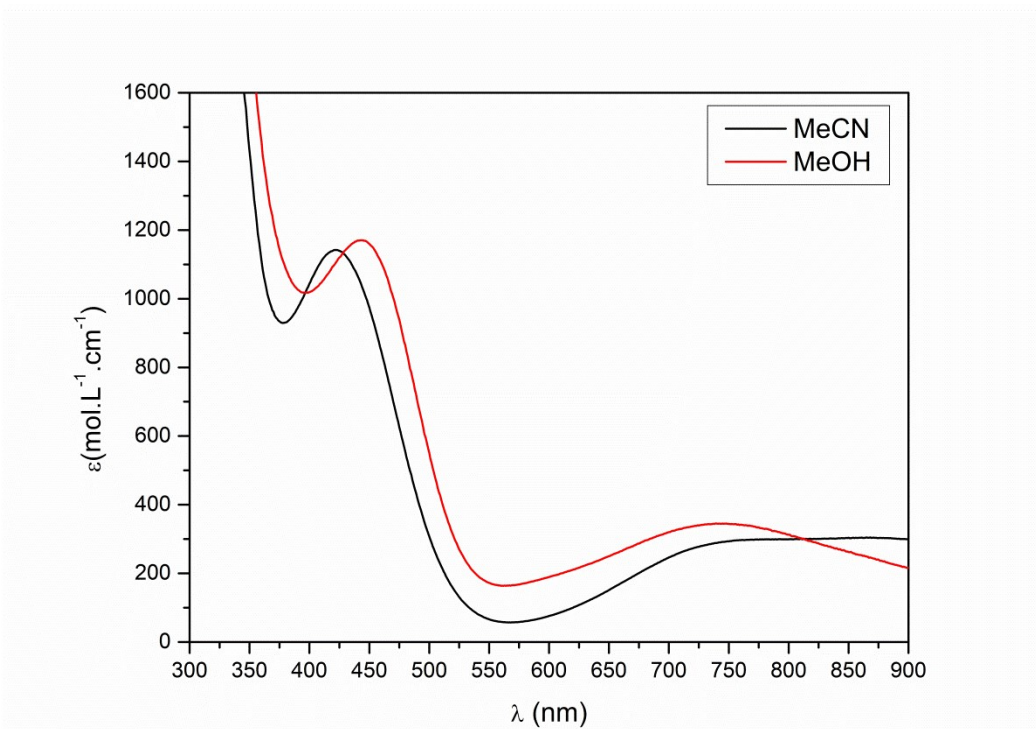
N1-C1 <sup>i</sup>	1.4770(18)	C6-H6	0.9500
N1-H1	0.8722	C7-C8	1.393(3)
C1-C2	1.515(2)	C7-H7	0.9500
C1-H1A	0.9900	C8-H8	0.9500
C1-H1B	0.9900	C1-C2-S1	111.60(11)
C2-S1	1.8303(17)	C1-C2-H2A	109.3
C2-H2A	0.9900	S1-C2-H2A	109.3
C2-H2B	0.9900	C1-C2-H2B	109.3
S1-C3	1.7797(17)	S1-C2-H2B	109.3
C3-C4	1.393(2)	H2A-C2-H2B	108.0
N1-Cu1-Cl1	164.92(6)	C3-S1-C2	102.00(7)
N1-Cu1-Cl2	96.60(6)	C3-S1-Cu1	115.06(5)
Cl1-Cu1-Cl2	98.48(2)	C2-S1-Cu1	96.47(5)
N1-Cu1-S1	81.774(19)	C4-C3-C8	119.96(16)
Cl1-Cu1-S1	93.720(12)	C4-C3-S1	123.06(12)
Cl2-Cu1-S1	107.228(11)	C8-C3-S1	116.95(13)
N1-Cu1-S1 <sup>i</sup>	81.774(19)	C5-C4-C3	119.46(16)
Cl1-Cu1-S1 <sup>i</sup>	93.720(12)	C5-C4-H4	120.3
Cl2-Cu1-S1 <sup>i</sup>	107.228(11)	C3-C4-H4	120.3
S1-Cu1-S1 <sup>i</sup>	143.18(2)	C6-C5-C4	120.58(17)
C1-N1-C1 <sup>i</sup>	114.10(17)	C6-C5-H5	119.7
C1-N1-Cu1	111.51(10)	C4-C5-H5	119.7
C1 <sup>i</sup> -N1-Cu1	111.51(10)	C7-C6-C5	119.99(18)
C1-N1-H1	106.9	C7-C6-H6	120.0
C1 <sup>i</sup> -N1-H1	106.9	C5-C6-H6	120.0
Cu1-N1-H1	105.3	C6-C7-C8	120.17(18)
N1-C1-C2	107.26(13)	C6-C7-H7	119.9
N1-C1-H1A	110.3	C8-C7-H7	119.9
C2-C1-H1A	110.3	C7-C8-C3	119.78(17)
N1-C1-H1B	110.3	C7-C8-H8	120.1
C2-C1-H1B	110.3	C3-C8-H8	120.1
H1A-C1-H1B	108.5		

Symmetry transformations used to generate equivalent atoms: (i) X, -Y+1.5, Z

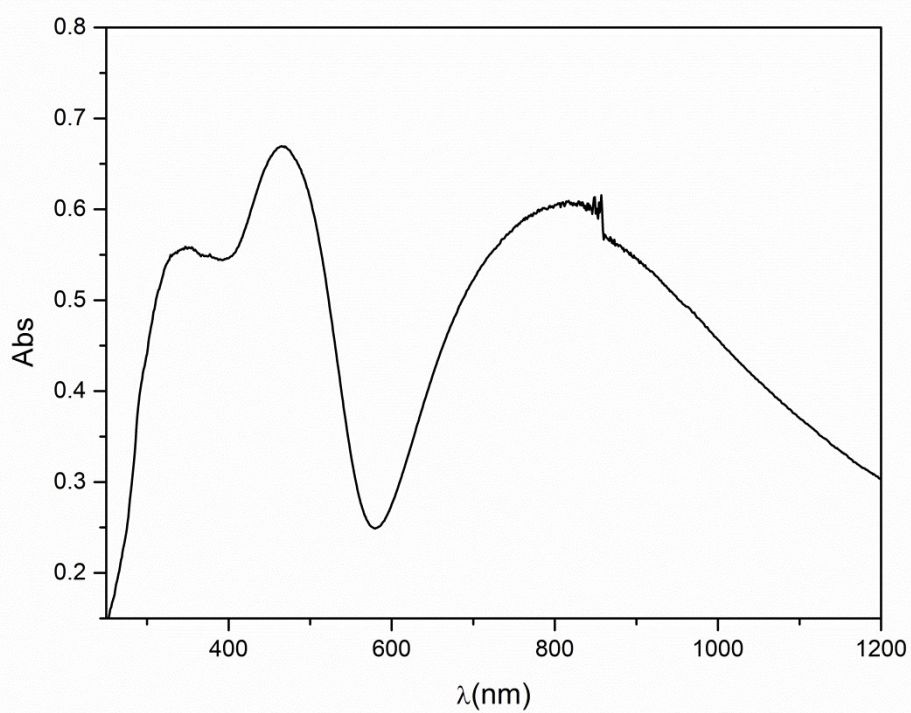




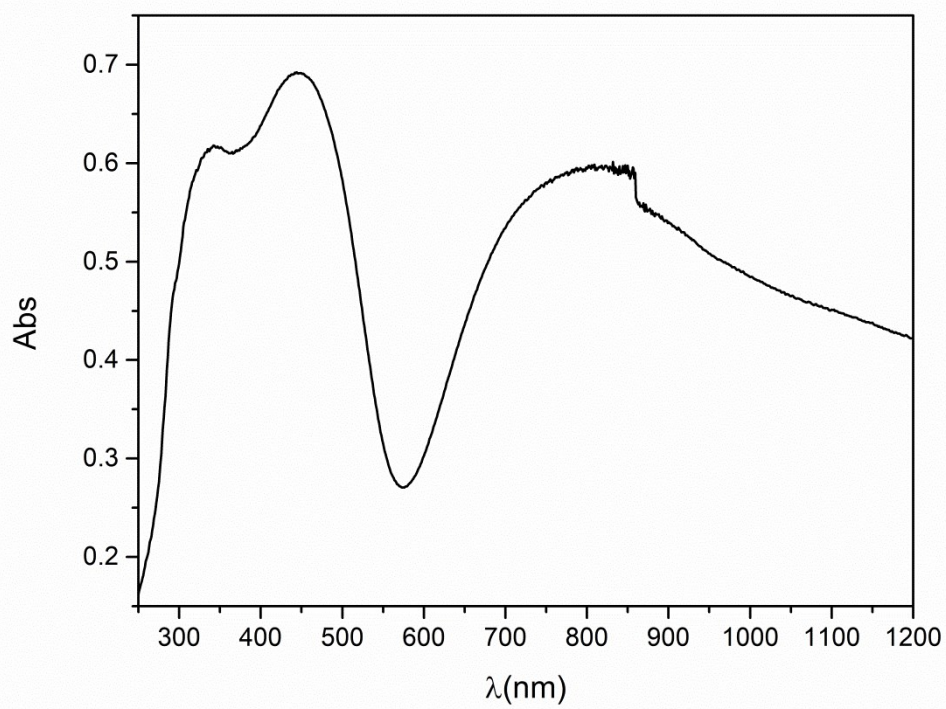
**Figure S10** Electronic spectrum of  $C_{Se}$  complex in acetonitrile solution in black and in methanol solution in red.



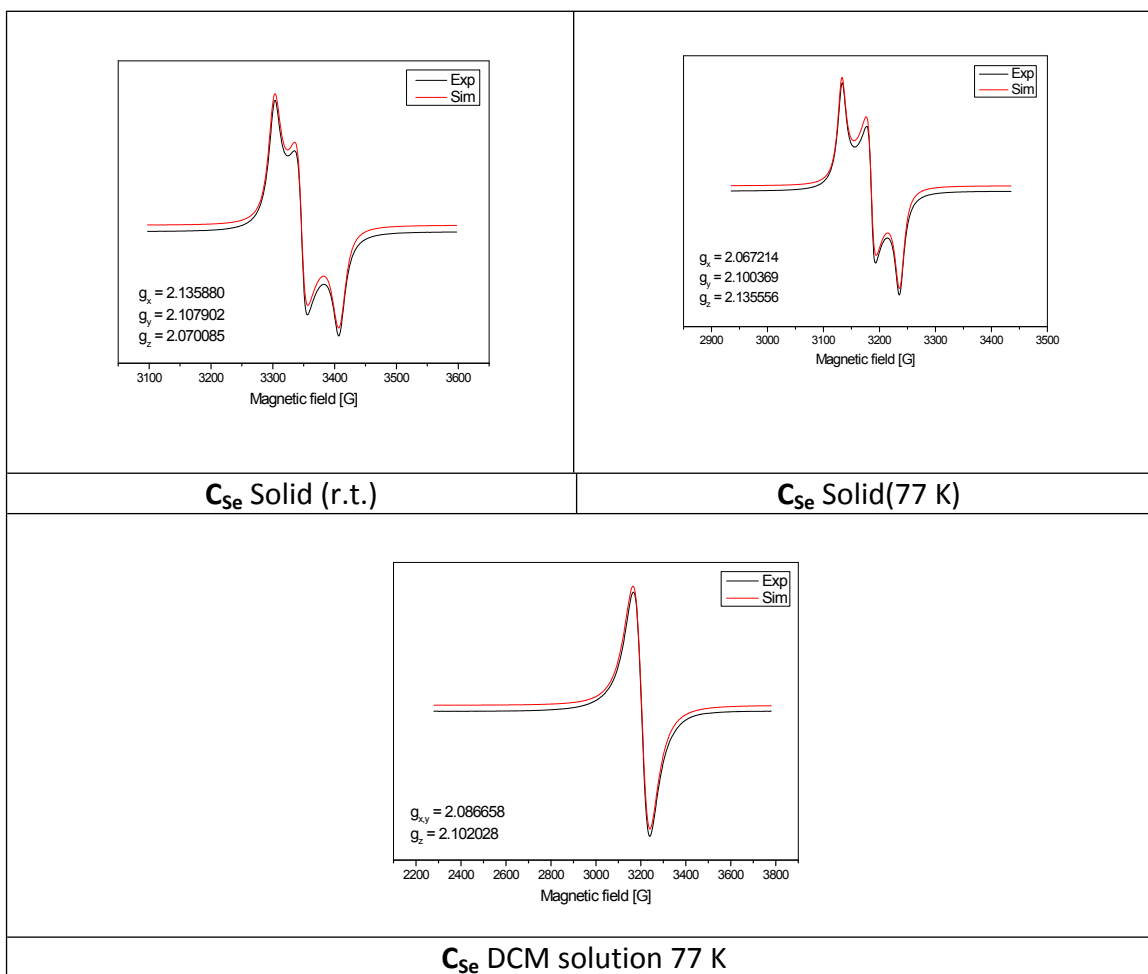
**Figure S11** Electronic spectrum of  $C_s$  complex in acetonitrile solution in black and in methanol solution in red.



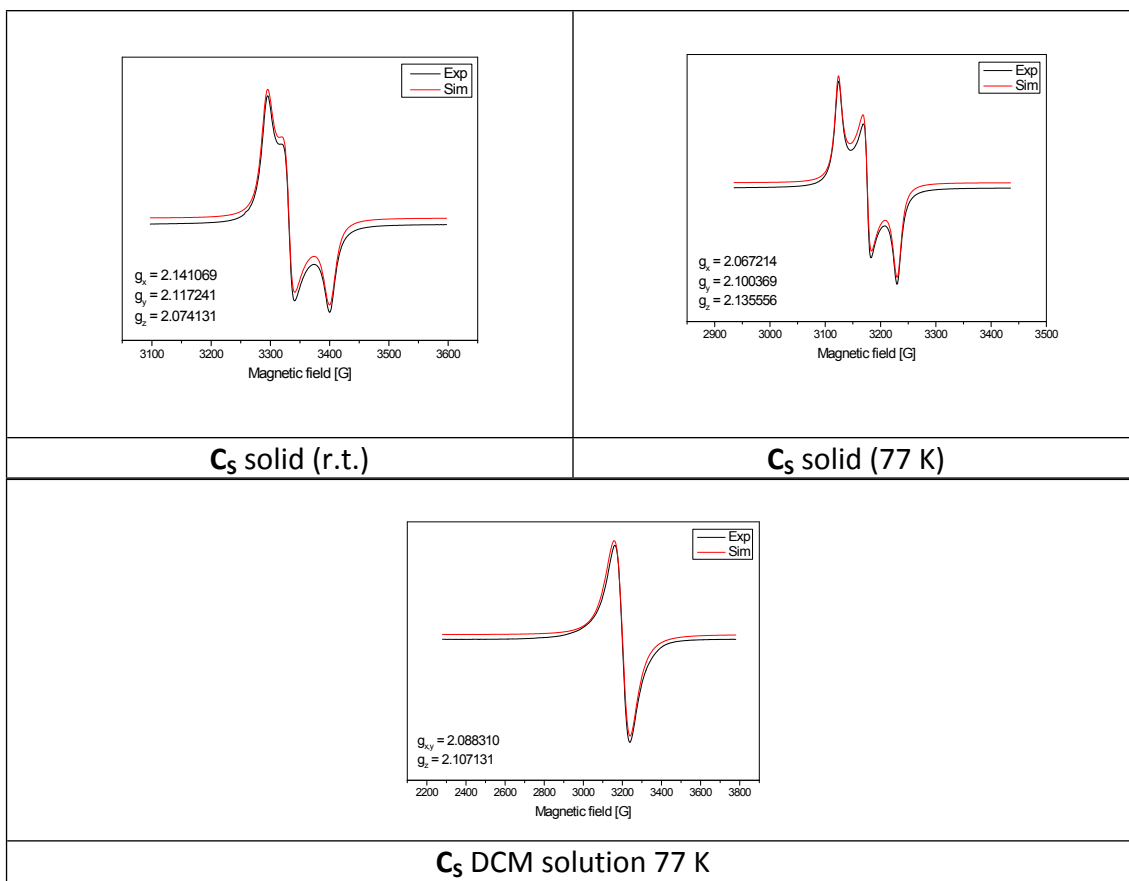
**Figure S12** Electronic spectrum of C<sub>Se</sub> in KBr pellet.



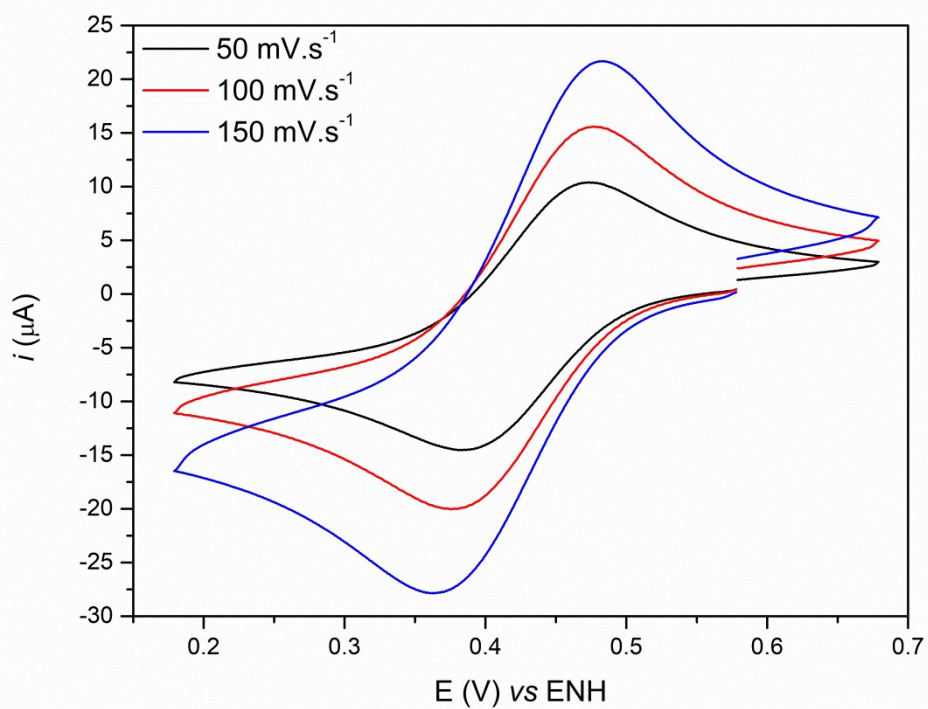
**Figure S13** Electronic spectrum of C<sub>S</sub> in KBr pellet.



**Figure S14** EPR Spectra of C<sub>Se</sub> complex.

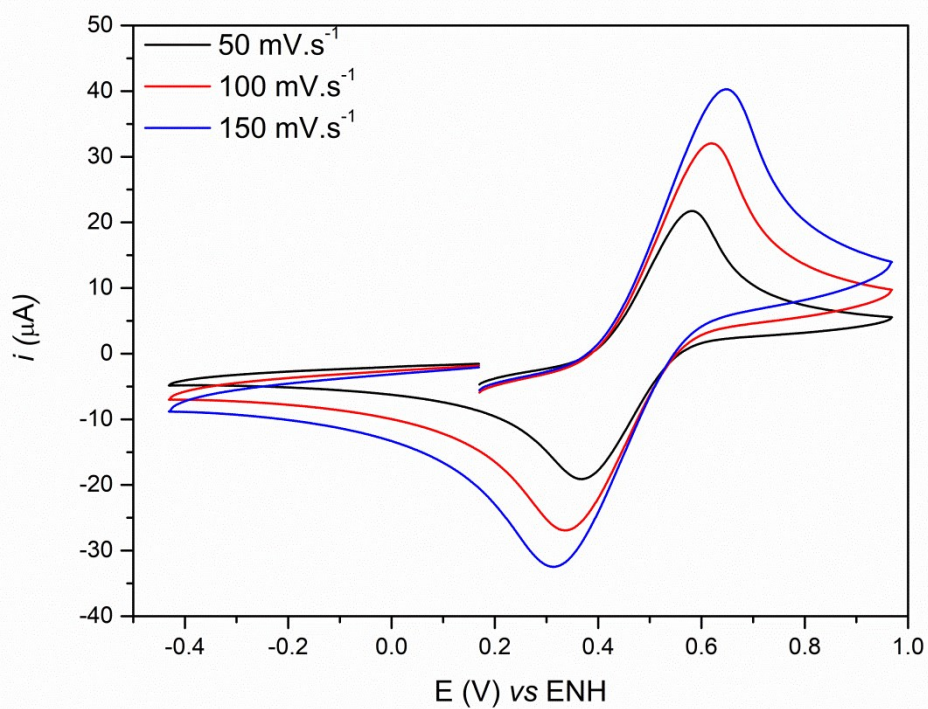


**Figure S15** EPR Spectra of C<sub>5</sub> complex.

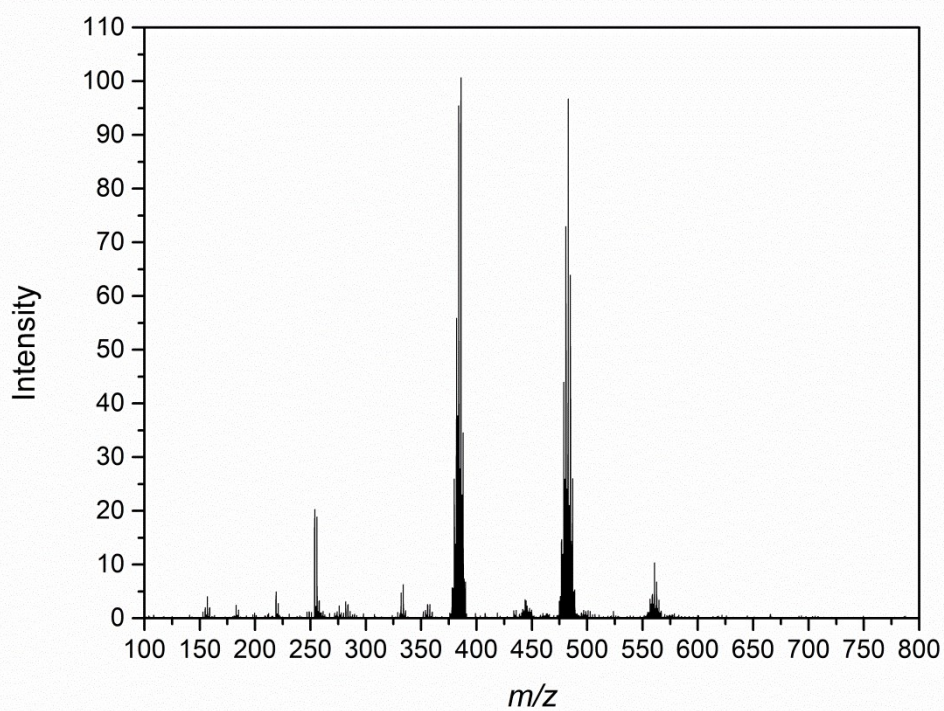


**Figure S16** Cyclic voltammetry of complex  $C_{se}$  in methanol. Conditions: working electrode (carbon); reference electrode ( $Ag/Ag^+$ ); auxiliary electrode (Pt); supporting electrolyte  $TBAPF_6$   $0.1 \text{ mol L}^{-1}$ .

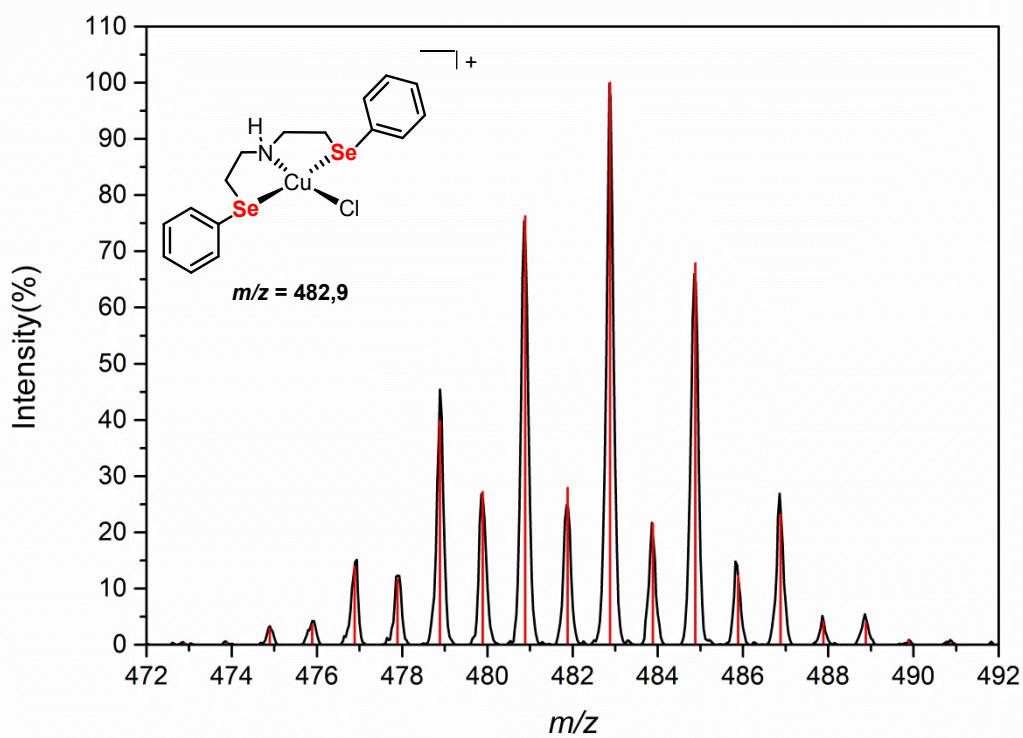




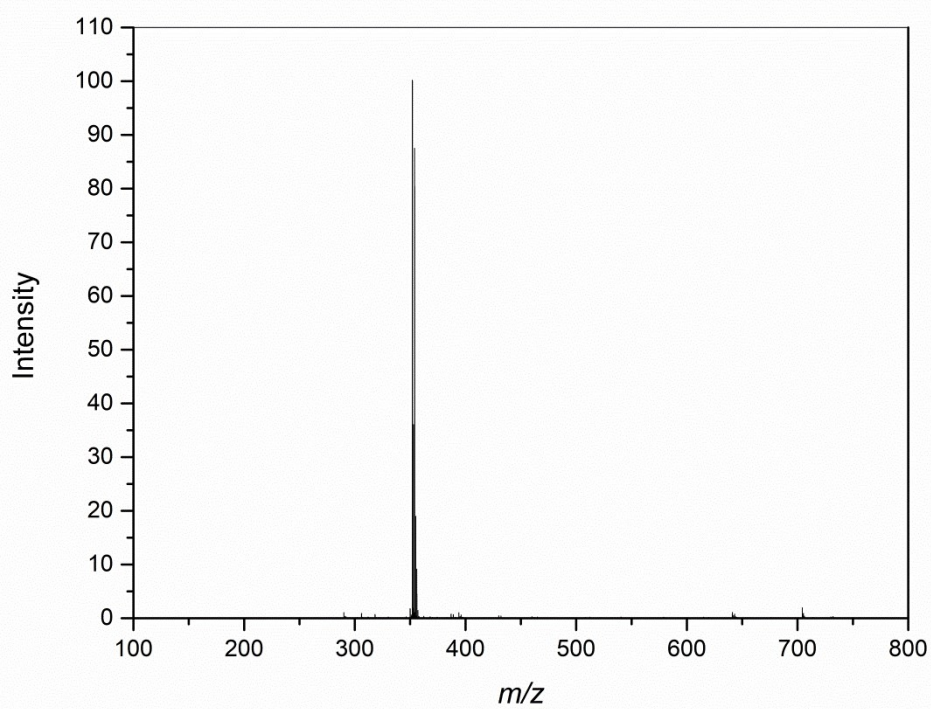
**Figure S17** Cyclic voltammetry of complex  $C_5$  in methanol. Conditions: working electrode (carbon); reference electrode ( $\text{Ag}/\text{Ag}^+$ ); auxiliary electrode (Pt); supporting electrolyte  $\text{TBAPF}_6$   $0.1 \text{ mol L}^{-1}$ .



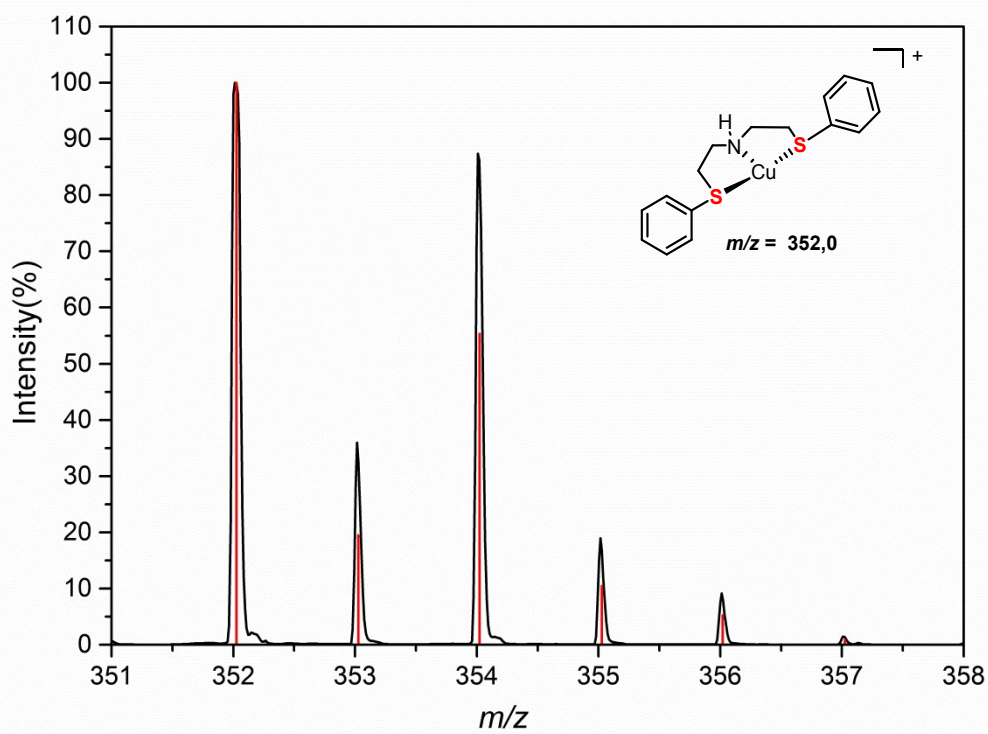
**Figure S18** ESI-MS spectrum (positive mode) in methanol of  $C_{Se}$ .



**Figure S19** Calculated (red) and experimental (black) isotopic distributions for the species present in the electrospray of  $C_{Se}$ .



**Figure S20** ESI-MS spectrum (positive mode) in methanol of  $C_5$ .





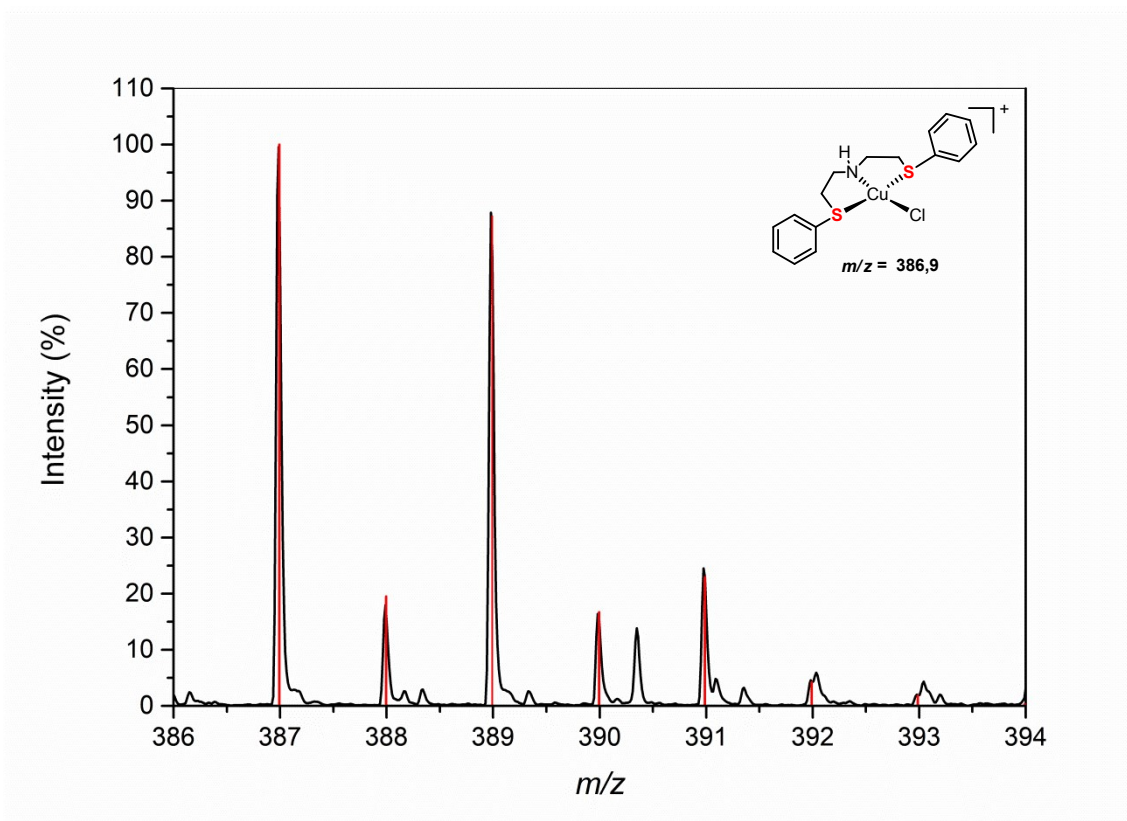


**Figure S21** Calculated (red) and experimental (black) isotopic distributions for the species present in the electrospray of  $C_S$ .

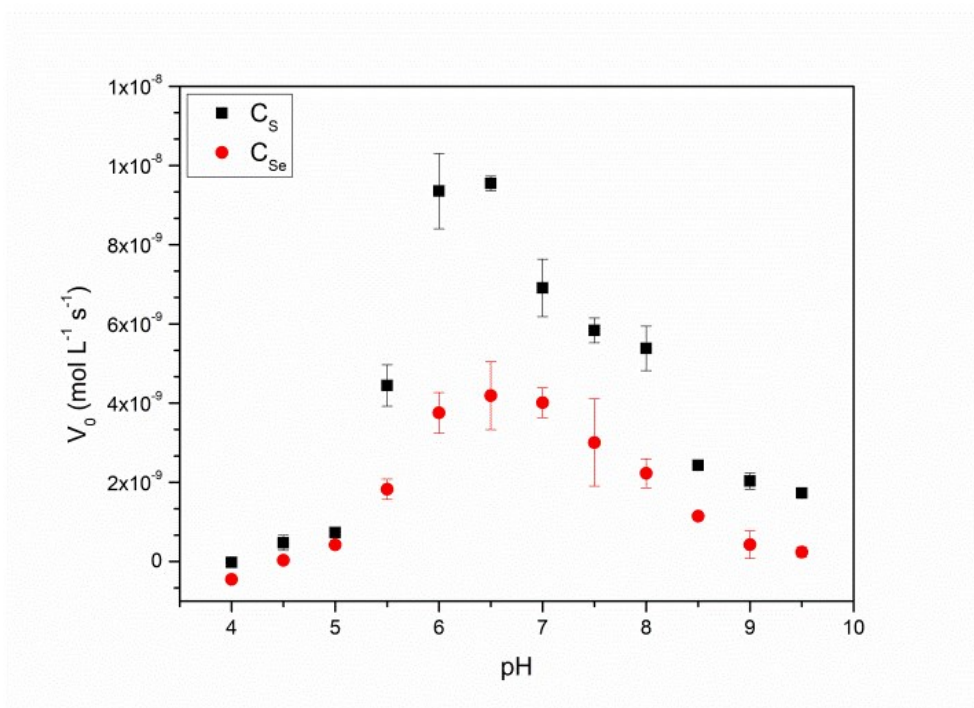


**Figure S 22** Graph showing the pH dependence in the hydrolysis of 2,4- BDNPP by complexes  $C_{Se}$  and  $C_S$ .

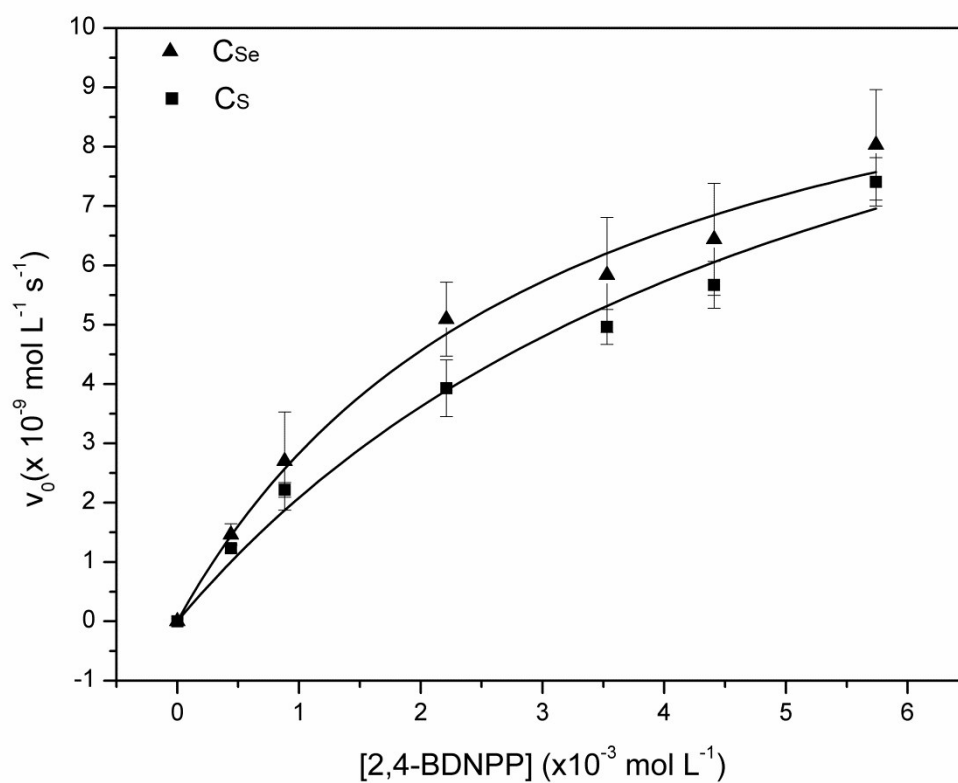


**Figure S 23** Dependence of substrate 2,4-BDNPP concentration for  $C_s$  and  $C_{Se}$  complexes at 25 ° C and pH 6.5. MeCN/H<sub>2</sub>O solution 50:50% v/v; [complex] =  $7.0 \times 10^{-5} \text{ mol L}^{-1}$ ; [substrate] =  $4.0 \times 10^{-4}$  to  $6.0 \times 10^{-3}$  and [Buffer]=  $0.05 \text{ mol L}^{-1}$ .

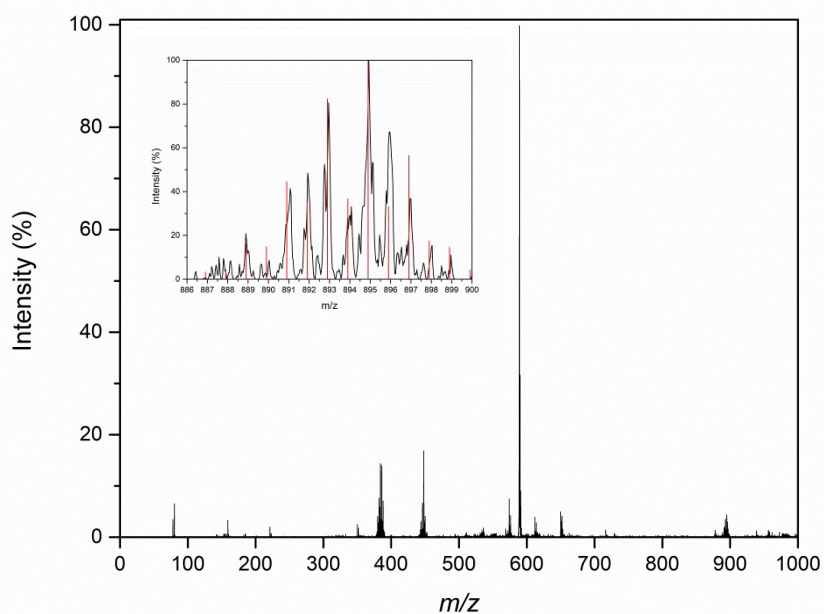


**Figure S24** ESI-MS analysis of the  $C_{se}$  in the presence of the substrate 2,4-BDNPP an acetonitrile/water (1:1, v/v), the expanding spectrum refers to the species:  $[Cu(L_{se})(OH)(2,4-BDNPP)] + H^+$

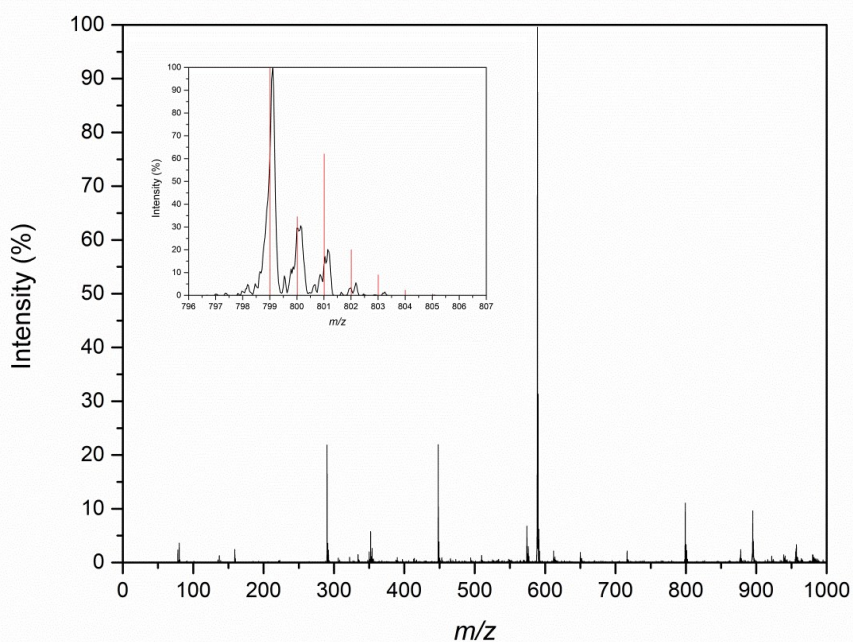


**Figure S25** ESI-MS analysis of the  $C_s$  in the presence of the substrate 2,4-BDNPP an acetonitrile/water (1:1, v/v), the expanding spectrum refers to the species:  $[Cu(L_s)(OH)(2,4-BDNPP)] + H^+$ .

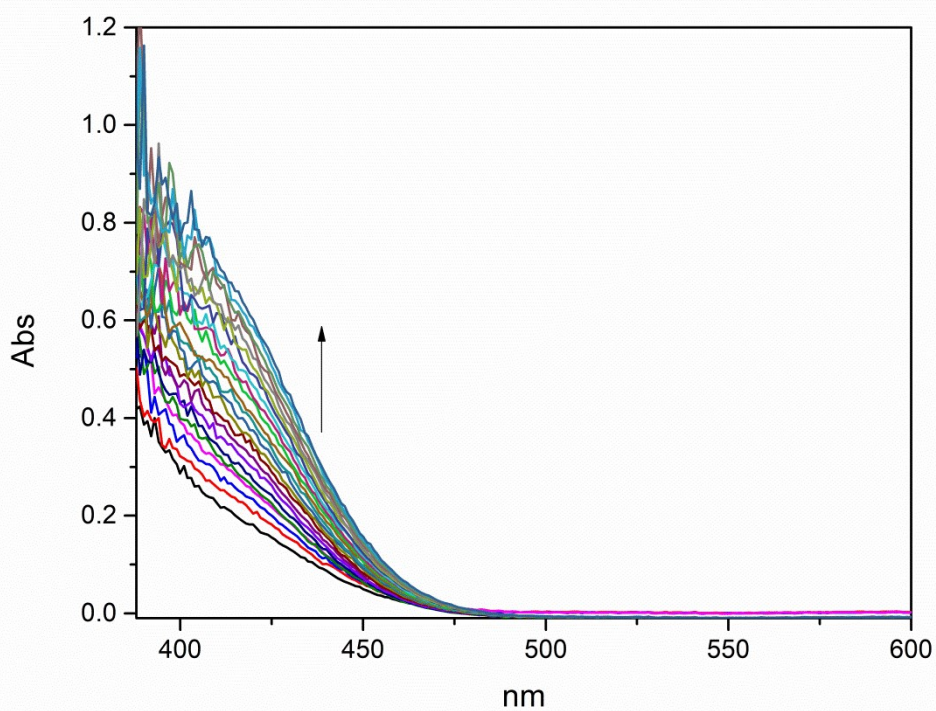


**Figure S26** Spectral variation observed during the hydrolysis of the substrate 2,4-BDNPP promoted by the  $C_5$  complex. Conditions: pH 6.5; 25 °C; MeCN / H<sub>2</sub>O solution (1: 1 v / v); [complex] =  $8.0 \times 10^{-5}$  mol L<sup>-1</sup>; [substrate] =  $8.0 \times 10^{-3}$  mol L<sup>-1</sup>; [buffer] = 0.05 mol L<sup>-1</sup>. The duration of the spectral variation experiment was 4 hours with an interval of 10 minutes between two spectral scans.

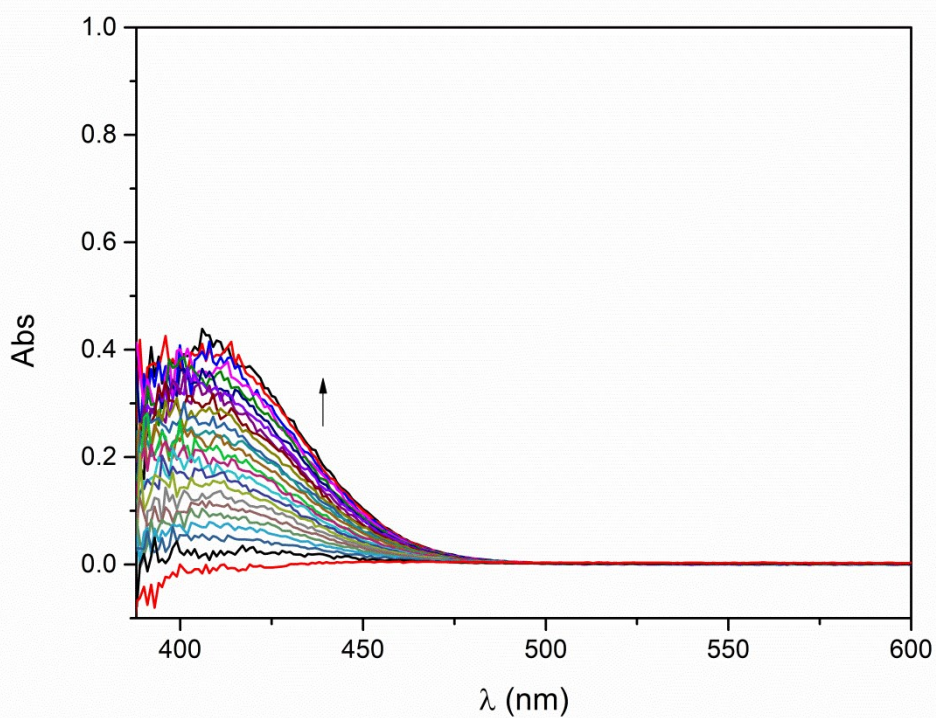


**Figure S27** Spectral variation observed during the hydrolysis of the substrate 2,4-BDNPP promoted by the  $C_{Se}$  complex. Conditions: pH 6.5; 25 °C; MeCN / H<sub>2</sub>O solution (1: 1 v / v); [complex] =  $8.0 \times 10^{-5}$  mol L<sup>-1</sup>; [substrate] =  $8.0 \times 10^{-3}$  mol L<sup>-1</sup>; [buffer] = 0.05 mol L<sup>-1</sup>. The duration of the spectral variation experiment was 4 hours with an interval of 10 minutes between two spectral scans.



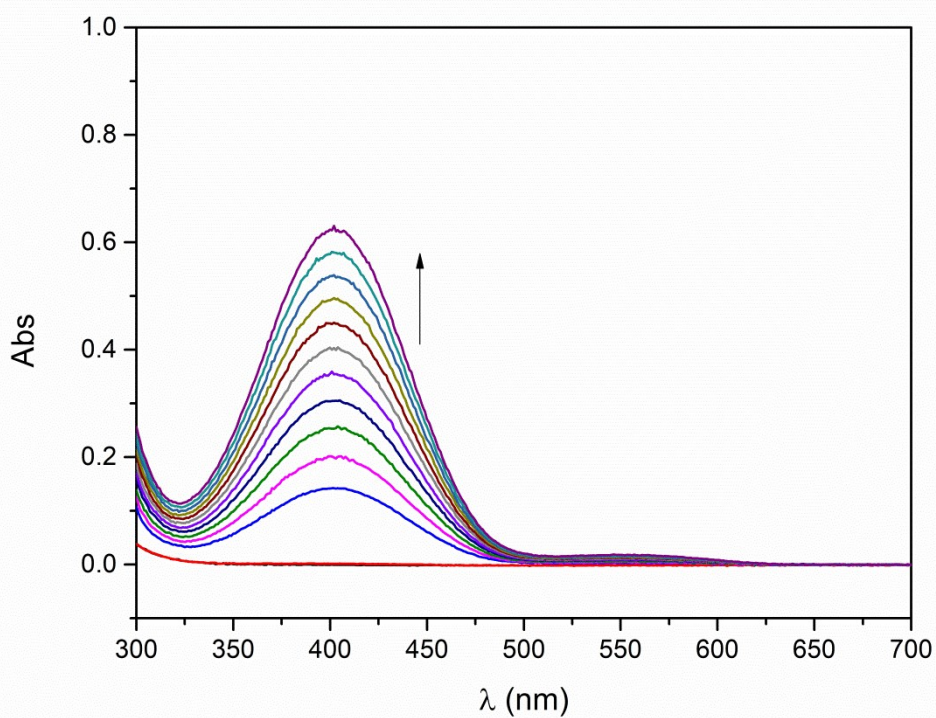


**Figure S28** Spectral variation observed during the oxidation of the substrate 3,5-DTBC promoted by the  $C_{Se}$  complex. Conditions: pH 7; 25 ° C; MeOH / H<sub>2</sub>O solution (97: 3% v / v); [complex] =  $3.0 \times 10^{-5}$  mol L<sup>-1</sup>; [substrate] =  $3.0 \times 10^{-3}$  mol L<sup>-1</sup>; [buffer] = 0.03 mol L<sup>-1</sup>. The duration of the spectral variation experiment was 1 hour with an interval of 5 minutes between two spectral scans.

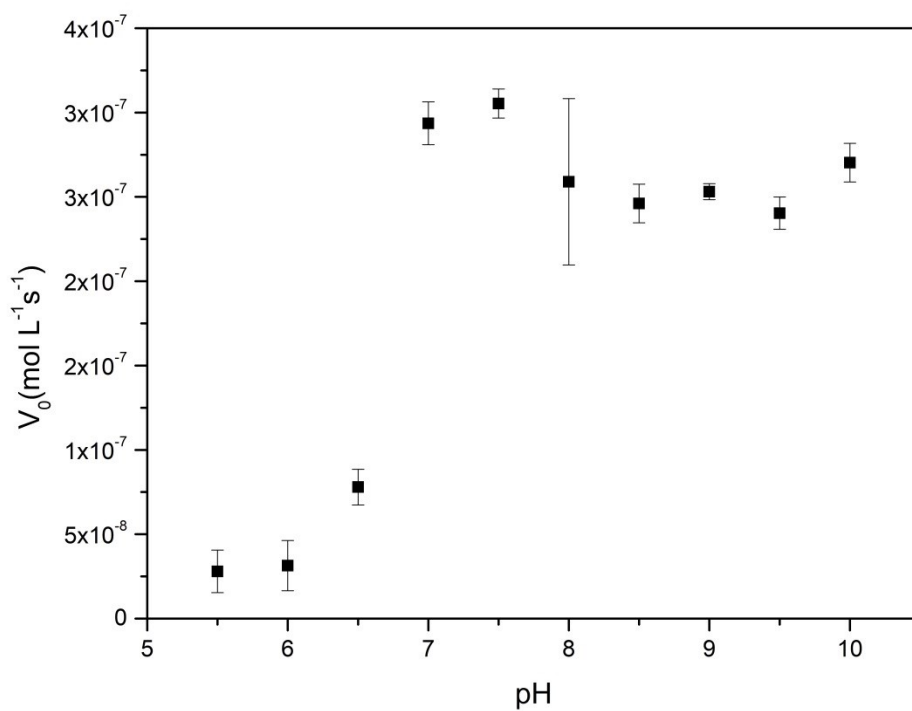


**Figure S29** Plots of  $v_0$  versus pH of  $C_{se}$  complex for 3,5-DTBC substrate oxidation reaction at 25 ° C. MeOH / H<sub>2</sub>O solution: 97: 3% v / v; [complex] =  $2.0 \times 10^{-5}$  mol L<sup>-1</sup>; [substrate] =  $2.4 \times 10^{-3}$  mol L<sup>-1</sup>; [buffer] = 0.03 mol L<sup>-1</sup>. (MES - pH 5.5 at 6.5, TRIS - pH 7.0 at 10.0).

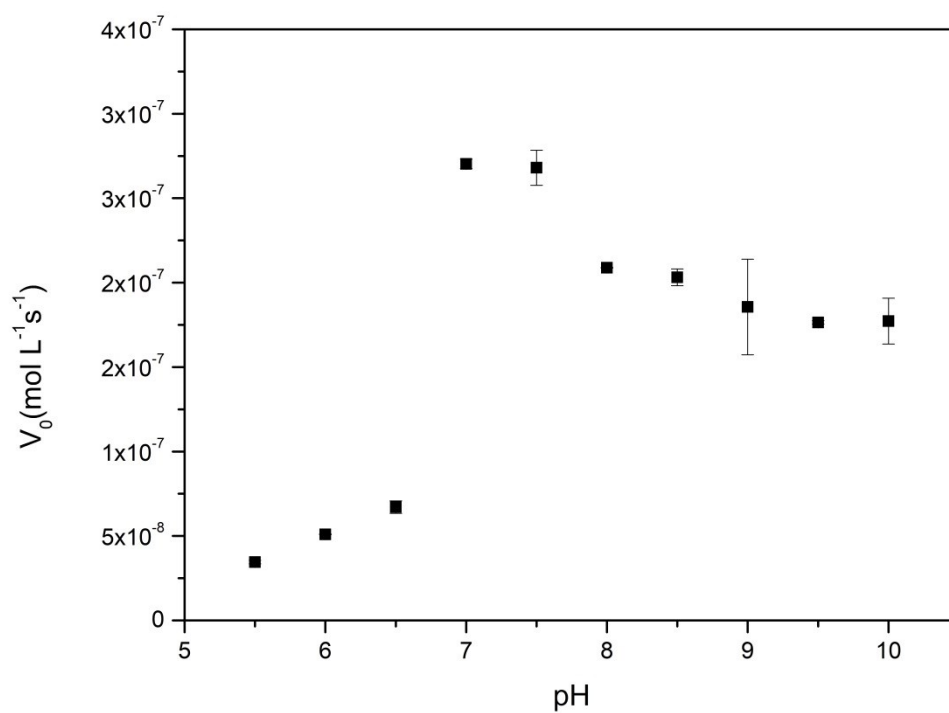


**Figure S30** Plots of  $v_0$  versus pH of  $C_S$  complex for 3,5-DTBC substrate oxidation reaction at 25 °C. MeOH / H<sub>2</sub>O solution 97: 3% v / v; [complex] =  $2.0 \times 10^{-5} \text{ mol L}^{-1}$ ; [substrate] =  $2.4 \times 10^{-3} \text{ mol L}^{-1}$ ; [buffer] =  $0.03 \text{ mol L}^{-1}$ . (MES - pH 5.5 at 6.5, TRIS - pH 7.0 at 10.0).

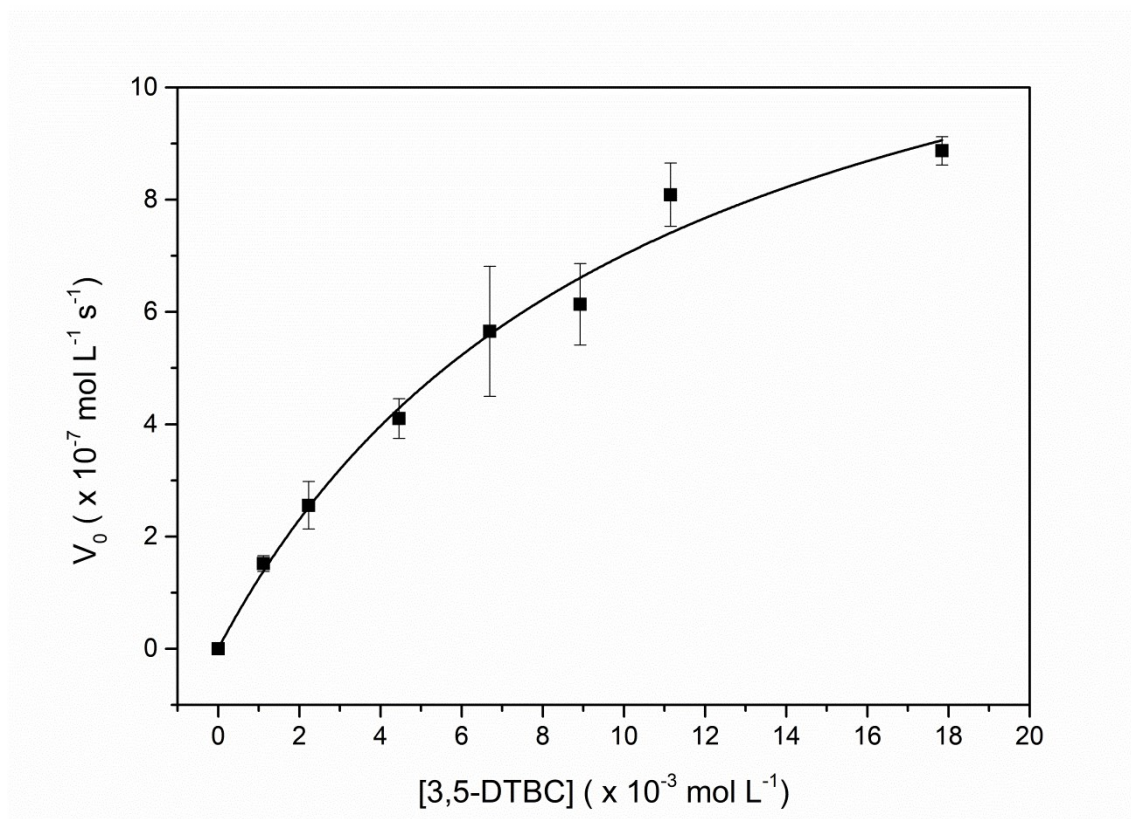


**Figure S31** Dependence on oxidation reaction rate of 3,5 - DTBC with substrate concentration for  $C_S$  complex at 25 °C and pH 7. MeOH / H<sub>2</sub>O solution 97:3% v / v; [complex] =  $3.3 \times 10^{-5} \text{ mol L}^{-1}$ ; [substrate] =  $11.15 \times 10^{-4}$  to  $17.84 \times 10^{-3} \text{ mol L}^{-1}$ ; [buffer] =  $0.03 \text{ mol L}^{-1}$ .



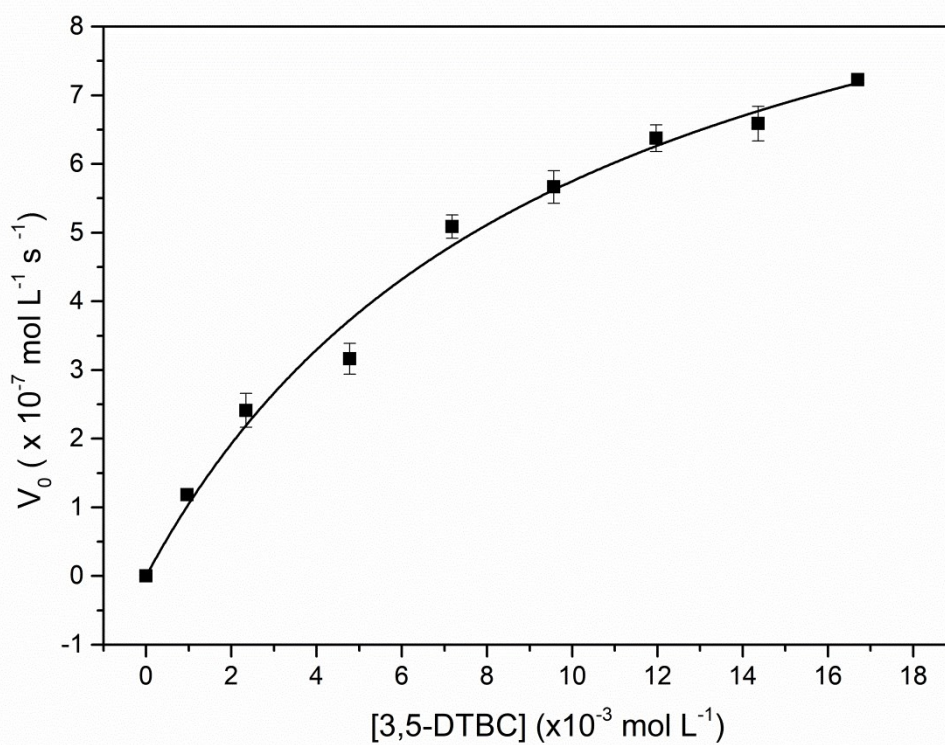


**Figure S32** Dependence on oxidation reaction rate of 3,5 - DTBC with substrate concentration for  $C_{Se}$  complex at 25 ° C and pH 7. MeOH / H<sub>2</sub>O solution 97: 3% v / v; [complex] =  $2.0 \times 10^{-5} \text{ mol L}^{-1}$ ; [substrate] =  $9.57 \times 10^{-4}$  to  $16.7 \times 10^{-3} \text{ mol L}^{-1}$ ; [buffer] =  $0.03 \text{ mol L}^{-1}$ .

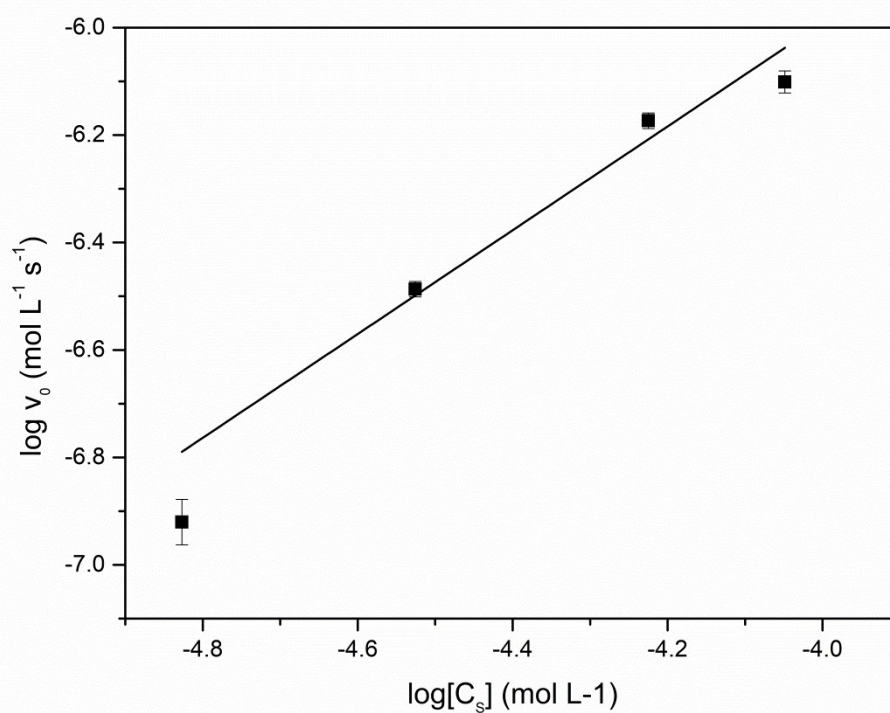


**Figure S33** Dependence on oxidation reaction rate of 3,5 - DTBC with substrate concentration for  $C_5$  complex at 25 °C and pH 7. MeOH / H<sub>2</sub>O solution 97: 3% v / v; [complex] =  $2.0 \times 10^{-5}$  mol L<sup>-1</sup>; [substrate] =  $9.0 \times 10^{-4}$  to  $1.6 \times 10^{-3}$  mol L<sup>-1</sup>; [buffer] = 0.03 mol L<sup>-1</sup>.

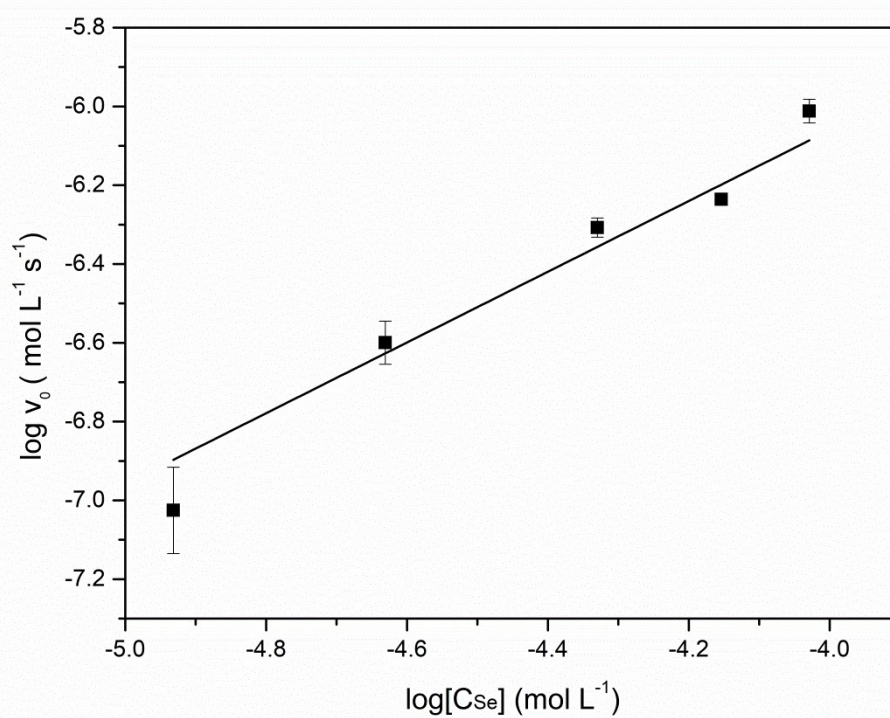


**Figure S34** Dependence on oxidation reaction rate of 3,5-DTBC with substrate concentration for  $C_{se}$  complex at 25 °C and pH 7. MeOH / H<sub>2</sub>O solution 97: 3% v / v; [complex] =  $2.0 \times 10^{-5}$  mol L<sup>-1</sup>; [substrate] =  $9.0 \times 10^{-4}$  to  $1.6 \times 10^{-3}$  mol L<sup>-1</sup>; [buffer] = 0.03 mol L<sup>-1</sup>.